# Extrapolating expected accuracies for recognition tasks

Charles Zheng, Rakesh Achanta and Yuval Benjamini

June 16, 2017

**Abstract**

The difficulty of multi-class classification generally increases with the number of classes. Using data from a subset of the classes, can we predict how well a classifier will scale with an increased number of classes? Under the assumption that the classes are sampled exchangeably, and under the assumption that the classifier is generative (e.g. QDA or Naive Bayes), we show that the expected accuracy when the classifier is trained on $k$ classes is the $k-1$st moment of a *conditional accuracy distribution*, which can be estimated from data. This provides the theoretical foundation for performance extrapolation based on pseudolikelihood, unbiased estimation, and high-dimensional asymptotics. We investigate the robustness of our methods to non-generative classifiers in simulations and one optical character recognition example.

## 1 Introduction

Human brains have a remarkable ability to recognize objects, faces, spoken syllables and words, and written symbols or words, and this recognition ability is essential for everyday life. While researchers in artificial intelligence have attempted to meet human benchmarks for these classical recognition tasks for the last few decades, only very recent advances in machine learning, such as deep neural networks, have allowed algorithmic recognition algorithms to approach or exceed human performance (LeCun, Bengio, and Hinton 2015).

Within the statistics and machine learning literature, the usual formalism for studying a recognition task is to pose it as a *multi-class classification* problem. One delineates a finite set of distinct entities which are to be recognized and distinguished, which is the *label set* $\mathcal{Y}$. The input data is assumed to take the form of a finite-dimensional real *feature vector* $X \in \mathbb{R}^p$. Each input instance is associated with exactly one true label $Y \in \mathcal{Y}$. The solution to the classification problem takes the form of an algorithmically implemented *classification rule* $h$ that maps vectors $X$ to predicted labels $\hat{Y} \in \mathcal{Y}$. The classification rule can be constructed in a data-dependent way: that is, one collects a number of labelled *training observations* $(X_1, Y_1)$ which is used to inform the construction of the classification rule $h$. The quality of the classification rule $h$ is measured by *generalization accuracy*

$$\mathrm{GA}(h) = \Pr[h(X) = Y],$$

where the probability is defined with reference to the unknown population joint distribution of $(X, Y)$.

However, a limitation of the usual multi-class classification framework for studying recognition problems is the assumption that the label set $\mathcal{Y}$ is finite and known in advance. When considering human recognition capabilities, it is clear that this is not the case. Our ability to recognize faces is not limited to some pre-defined, fixed set of faces; same with our ability to recognize objects in the environment. Humans learn to recognize novel faces and objects on a daily basis. And, if artificial intelligence is to fully match the human capability for recognition, it must also possess the ability to add new categories of entities to its label set over time; however, at present, there currently exists a void in the machine learning literature on the subject of the online learning of new classes in the data.

The central theme of this thesis is the study of *randomized classification*, which can be motivated as an extension of the classical multi-class classification framework to accommodate the possibility of growing or infinite label sets $\mathcal{Y}$. The basic approach taken is to assume an infinite or even continuous label space $\mathcal{Y}$, and then to study the problem of classification on finite label sets $S$ which are randomly sampled from $\mathcal{Y}$. This, therefore defines a *randomized classification* problem where the label set is finite but may vary from instance to instance. One can then proceed to answer questions about the variability of the performance due to randomness in the labels, or how performance changes depending on the size of the random label set.

# 2 Randomized classification

## 2.1 Motivation

The formalism of classification is inadequate for studying many practical questions related to the generalizability of the facial recognition system. Using test data, we estimate the generalization accuracy of a recognition system. However, these estimated accuracies apply only to the particular collection of individuals $\{y^{(1)}, \ldots, y^{(k)}\}$. If we were to add a new individual $y^{(k+1)}$ to the dataset, for instance, when photographs are uploaded on Facebook containing a new user, this defines a totally new classification problem because the expanded set of labels $\{y^{(1)}, \ldots, y^{(k+1)}\}$ defines a different response space than the old set of labels $\{y^{(1)}, \ldots, y^{(k)}\}$. Yet, these two classification problems are clearly linked. To take another example, a client might want to run a facial recognition system developed by lab A on their own database of individuals. In this case, there might be no overlap between the people in lab A's database and the people in the client's database. And yet, the client might still expect the performance figures reported by lab A to be informative of how well the recognition system will do on their own database!

The question of how to link performance between two different but related classification tasks is an active area of research, known as *transfer learning*. But while the two examples we just listed might be considered as examples of transfer learning problems, the current literature on transfer learning, as far as we know, does not study the problem of *mutating label sets*. Therefore, to address this new class of questions about the generalizability of the recognition system, we need to formalize our notions of (a) what constitutes a 'recognition system' which can be applied to different classification problems, and (b) what assumptions about the problem, and what assumptions about the classifiers used, allow one to infer performance in one classification problem based on performance in another classification problem.

## 2.2 Setup

By 'recognition system,' we really mean a *learning algorithm* $\Lambda$ which can take training data as input, and produce a classification rule for recognizing faces. While a classification rule is bound to a specific label set, a learning algorithm can be applied to datasets with arbitrary label sets, and be continually updated as new labels are added to the label set. To 'update' a facial recognition system with new data means to apply the learning algorithm to the updated database.

Now we can formalize what it means to generalize performance from one problem to another. A *classification problem* $P$ is specified by a label set $\mathcal{Y}$, a predictor space $\mathcal{X}$, a joint distribution $G$ on $\mathcal{X} \times \mathcal{Y}$, and a *sampling scheme* $S$ for obtaining training data (for example, to obtain $n$ observations from $G$ i.i.d.). The sampling scheme is needed because we cannot say much about how the learning algorithm will perform unless we know how much training data it is going to have. The generalization accuracy (GA) of the algorithm $\Lambda$ on the classification problem $P = (\mathcal{Y}, \mathcal{X}, G, S)$ is defined as the expected risk of the resulting classification rule $h$,

$$\mathrm{GA}_P(\Lambda) = \mathbf{E}[\mathrm{GA}(h)]$$

where $h$ is produced by applying $\Lambda$ to the training data, sampled by $S$. The expectation is taken over the randomness in the generation of the training data.

At this point we have defined an extremely general transfer learning problem: given two different classification problems $P_1 = (\mathcal{Y}_1, \mathcal{X}_1, G_1, S_1)$ and $P_2 = (\mathcal{Y}_2, \mathcal{X}_2, G_2, S_2)$, what can we say about the relationship between $\mathrm{GA}_{P_1}(\Lambda)$ and $\mathrm{GA}_{P_2}(\Lambda)$? Not much, unless we make many more assumptions about how $P_1$ and $P_2$ are linked.

The basic approach we will take is to assume that both $P_1$ and $P_2$ have been generated randomly via a common mechanism. In the original motivating context of facial recognition, this is to say that two different label sets $\mathcal{Y}_1$ and $\mathcal{Y}_2$ are linked because they both belong to a common population of labels $\mathcal{Y}$, i.e., the population of all possible humans, and to further assume that both have been *sampled*, in the same manner, from $\mathcal{Y}$.

The study of how to make inferences about the risk in $P_2$ given information about the performance achieved in $P_1$, granted a set of assumptions on how $P_1$ and $P_2$ have been randomly generated (and are thereby linked through shared randomization mechanisms) forms the basis of the subject of *randomized classification*.

As we noted in the introduction, the problem of randomized classification has a close ancestor in the study of *random code models* in information theory. There, the problem is to understand the *decoding performance* (the analogue to risk) of a encoding/decoding system $P$ which has a randomized code space $\mathcal{Y}$. Where random code models have a random codebook which is a sample over a distribution of all possible codes, randomized classification problems have a random label set that is a sample of a larger label space. However, the results we obtain for randomized classification are more general in nature than the existing results availible for random code models, because work on random codes is generally limited to asymptotic settings, whereas we obtain finite-$k$ results, and because random code models assume a specific product-distribution structure on $(X, Y)$ which is not appropriate for classification problems.

## 2.3 Assumptions

The randomized classification model we study has the following features. We assume that there exists an infinite (or even continuous) label space $\mathcal{Y}$ and a response space $\mathcal{X} \in \mathbb{R}^p$. For each label $y \in \mathcal{Y}$, there exists a distribution of features $F_y$. That is to say, that for a feature-label pair $(X, Y)$, that the conditional distribution of $X$ given $Y = y$ is given by $F_y$. Furthermore, we assume that there exists a prior distribution $\pi$ on the label space $\mathcal{Y}$.

A random classification task $P$ can be generated as follows. The label set $\mathcal{S} = \{Y^{(1)}, \ldots, Y^{(k)}\}$ is generated by drawing labels $Y^{(1)}, \ldots, Y^{(k)}$ i.i.d. from $\pi$. The joint distribution $G$ of pairs $(X, Y)$ is uniquely specified by the two conditions that (i) the marginal distribution of $Y$ is uniform over $\mathcal{S}$, and (ii) the conditional distribution of $X$ given $Y = Y^{(i)}$ is $F_{Y^{(i)}}$. We sample both a training set and a test set. The training set is obtained by sampling $r_1$ observations $X^{(i)}_{j,train}$ i.i.d. from $F_{Y^{(i)}}$ for $j = 1, \ldots, r_1$. The test set is likewise obtained by sampling $r_2$ observations $X^{(i)}_j$ i.i.d. from $F_{Y^{(i)}}$ for $j = 1, \ldots, r_2$. For notational convenience, we represent the training set as the set of empirical distributions $\{\hat{F}_{Y^{(i)}}\}_{i=1}^k$ where

$$\hat{F}_{Y^{(i)}} = \frac{1}{r_1} \sum_{j=1}^{r_1} \delta_{X^{(i)}_{j,train}}.$$

Figure 1 illustrates the sampling scheme for generating the training set.

Our analysis will also rely on a property of the classifier. We do not want the classifier to rely too strongly on complicated interactions between the labels in the set. We therefore propose the following property of marginal separability for classification models:

**Definition 2.1** *1. The classification rule $h$ is called a* marginal rule *if*

$$h(x) = argmax_{y \in \mathcal{S}} m_y(x),$$

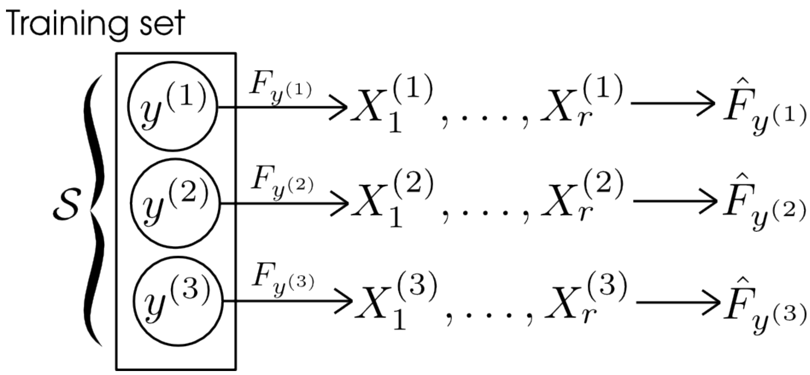


Figure 1: Training set

*where the function* $m_y$ *maps* $\mathcal{X}$ *to* $\mathbb{R}$.

2. *Define a marginal model* $\mathcal{M}$ *as a mapping from empirical distributions to margin functions,*
$$\mathcal{M}(\hat{F}_y) = m_y(x).$$

3. *A classifier that produces marginal classification rules*
$$h(x) = argmax_{y \in \mathcal{S}} m_y(x),$$
*by use of a marginal model, i.e. such that* $m_y = \mathcal{M}(\hat{F}_y)$ *for some marginal model* $\mathcal{M}$*, is called a* marginal classifier*.*

In words, a marginal classification rule produces a *margin*, or score, for each label, and chooses the label with the highest margin. The marginal model converts empirical distributions $\hat{F}_y$ over $\mathcal{X}$ into the margin function $m_y$. The *marginal* property allows us to prove strong results about the accuracy of the classifier under i.i.d. sampling assumptions.

**Comments:**

1. The marginal model includes several popular classifiers. A primary example for a marginal model is the estimated Bayes classifier. Let $\hat{f}_y$ be a density estimate obtained from the empirical distribution $\hat{F}_y$. Then, we can use the estimated densities of each class to produce the margin functions:
$$m_y^{EB}(x) = \log(\hat{f}_y(x)).$$

The resulting empirical approximation for the Bayes classifier (further assuming a uniform prior $\pi$) would be

$$f^{EB}(x) = \text{argmax}_{y \in \mathcal{S}}(m_y^{EB}(x)).$$

2. Both the Quadratic Discriminant Analysis and the naive Bayes classifiers can be seen as specific instances of an estimated Bayes classifier [1]. For QDA, the margin function is given by

$$m_y^{QDA}(x) = -(x - \mu(\hat{F}_y))^T \Sigma(\hat{F}_y)^{-1}(x - \mu(\hat{F}_y)) - \log\det(\Sigma(\hat{F}_y)),$$

where $\mu(F) = \int y dF(y)$ and $\Sigma(F) = \int (y - \mu(F))(y - \mu(F))^T dF(y)$. In Naive Bayes, the margin function is

$$m_y^{NB}(x) = \sum_{i=1}^{n} \log \hat{f}_{y,i}(x),$$

where $\hat{f}_{y,i}$ is a density estimate for the $i$-th component of $\hat{F}_y$.

3. There are also many classifiers which do not satisfy the marginal property, such as multinomial logistic regression, multilayer neural networks, decision trees, and k-nearest neighbors.

The operation of a marginal classifier is illustrated in figure 2. Since a marginal classifier is specified entirely by its marginal model $\mathcal{M}$, we will take the notational convention of referring to a marginal classifier as $\mathcal{M}$.

We would like to identify the sources of randomness in evaluating a classifier. First, there is the specific choice of $k$ classes for the label set. Second, there is randomness in training the classifier for these classes, which comes from the use of a finite training set. Third, there is the randomness in the estimated risk when testing the classifier on a test set.

If we *fix* a particular realization of the random label set $\mathcal{S} = \{y^{(1)}, \ldots, y^{(k)}\}$ as well as the training set $\{\hat{F}_{y^{(i)}}\}_{i=1}^k$, then the classifier $h(x)$ is fixed, and only

[1] QDA is the special case of the estimated Bayes classifier when $\hat{f}_y$ is obtained as the multivariate Gaussian density with mean and covariance parameters estimated from the data. Naive Bayes is the estimated Bayes classifier when $\hat{f}_y$ is obtained as the product of estimated componentwise marginal distributions of $p(x_i|y)$

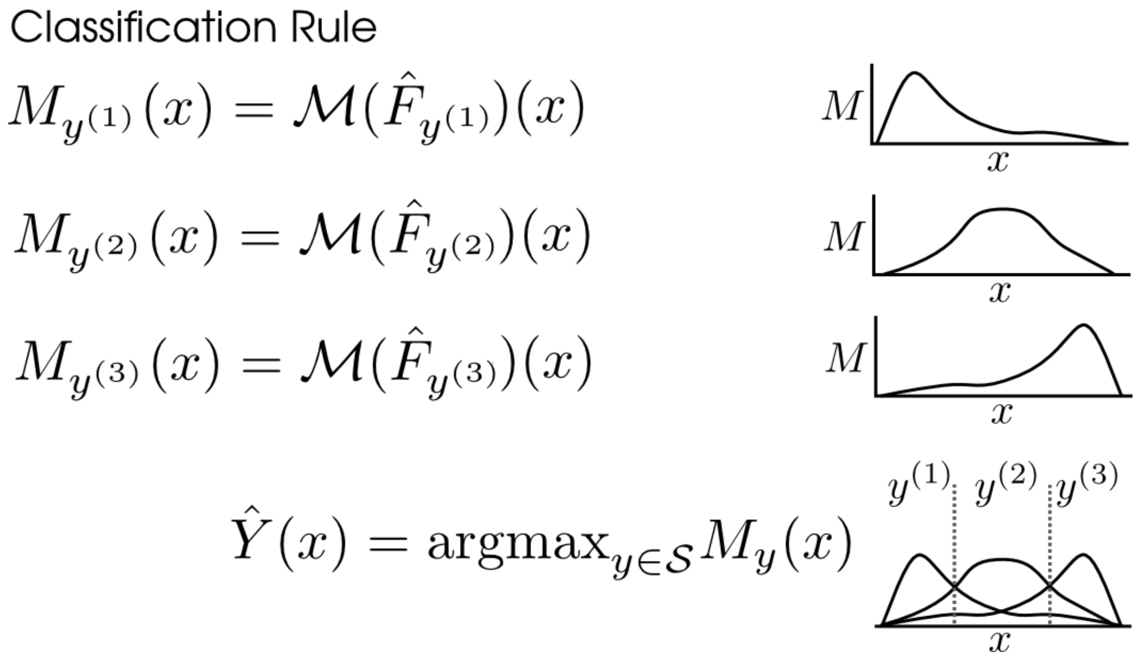


Figure 2: Classification rule

the third source of randomness (in test risk) applies. However, the true generalization accuracy of the classifier is deterministic:

$$
\begin{aligned}
\text{GA}(h) &= \Pr[Y = h(X) | Y \sim \text{Unif}(\mathcal{S}), \mathcal{S}, \{\hat{F}_{y^{(i)}}\}_{i=1}^k] \\
&= \frac{1}{k} \sum_{i=1}^k \Pr[m_{y^{(i)}}(x) = \max_j m_{y^{(j)}}(x) | X \sim F_{y^{(i)}}, \mathcal{S}, \{\hat{F}_{y^{(i)}}\}_{i=1}^k]. \\
&= \frac{1}{k} \sum_{i=1}^k \int_{\mathcal{X}} I(m_{y^{(i)}}(x) = \max_j m_{y^{(j)}}(x)) dF_{y^{(i)}}(x),
\end{aligned}
$$

recalling that $m_{y^{(i)}}(x) \stackrel{def}{=} \mathcal{M}(\hat{F}_{y^{(i)}})(x)$ is the margin function obtained from the training data of the $i$th class.

If we *fix* a particular realization of the random label set $\mathcal{S} = \{y^{(1)}, \ldots, y^{(k)}\}$, then we can define the (generalization) accuracy specific to that label set. However, the training data $\{\hat{F}_{y^{(i)}}\}_{i=1}^k$ will be random. Let us denote the *distribution* of the empirical distribution $\hat{F}_y$ constructed from sample size $r$ as

$\Pi_{y,r}$. The accuracy of the classifier $\mathcal{M}$ on label set $\mathcal{S}$ is given by

$$\begin{aligned}\mathrm{GA}_{\mathcal{S}}(\mathcal{M}) &= \Pr[Y = h(X)|Y \sim \mathrm{Unif}(\mathcal{S}), \hat{F}_{y^{(i)}} \sim \Pi_{y^{(i)},r_1}] \\ &= \frac{1}{k}\sum_{i=1}^k \int I(\mathcal{M}(\hat{F}_{y^{(i)}})(x) = \max_j \mathcal{M}(\hat{F}_{y^{(j)}})(x))dF_{y^{(i)}}(x)\prod_{\ell=1}^k d\Pi_{y^{(\ell)},r_1}(\hat{F}_{y^{(\ell)}}).\end{aligned}$$

The calculation of the accuracy (for fixed label set $\mathcal{S}$) is illustrated in figure 3.

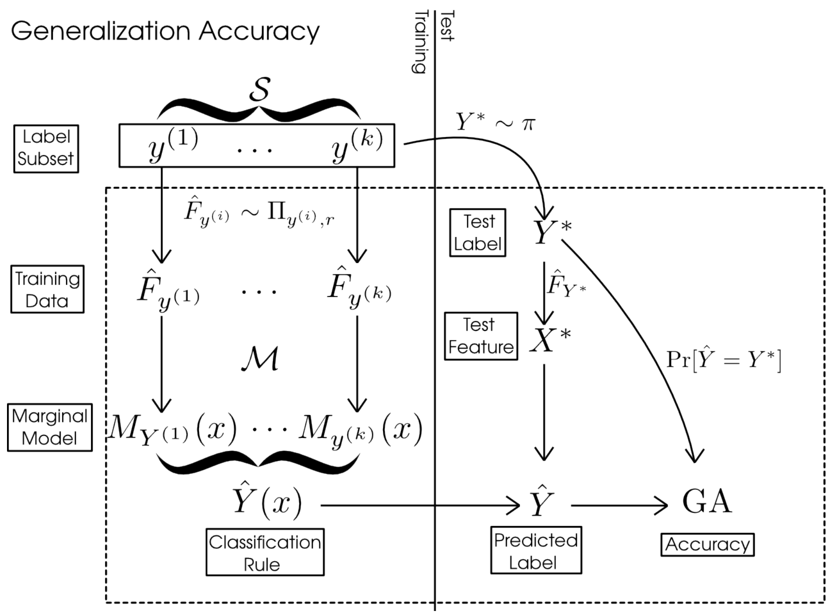


Figure 3: Generalization accuracy

Finally, suppose we do not fix any of the random quantities in the classification task $P$, and merely specify $k$, the number of classes, and $r_1$, the number of repeats in the training set. Then the $k$-class, $r$-repeat *average generalization accuracy* of a marginal classifier $\mathcal{M}$ is defined as

$$\begin{aligned}\mathrm{AGA}_{k,r_1}(\mathcal{M}) &= \mathbf{E}[\mathrm{GA}_{\mathcal{S}}(\mathcal{M})|Y^{(1)},\ldots,Y^{(k)} \sim \pi] \\ &= \frac{1}{k}\sum_{i=1}^k \int I(\mathcal{M}(\hat{F}_{y^{(i)}})(x) = \max_j \mathcal{M}(\hat{F}_{y^{(j)}}))dF_{y^{(i)}}(x)\prod_{\ell=1}^k d\Pi_{y^{(\ell)},r_1}(\hat{F}_{y^{(\ell)}})d\pi(y^{(\ell)}). \\ &= \int I(\mathcal{M}(\hat{F}_{y^{(1)}})(x) = \max_j \mathcal{M}(\hat{F}_{y^{(j)}}))dF_{y^{(1)}}(x)\prod_{\ell=1}^k d\Pi_{y^{(\ell)},r_1}(\hat{F}_{y^{(\ell)}})d\pi(y^{(\ell)}).\end{aligned}$$

where the last line follows from noting that all $k$ summands in the previous line are identical. The definition of average generalization accuracy is illustrated in Figure 4.

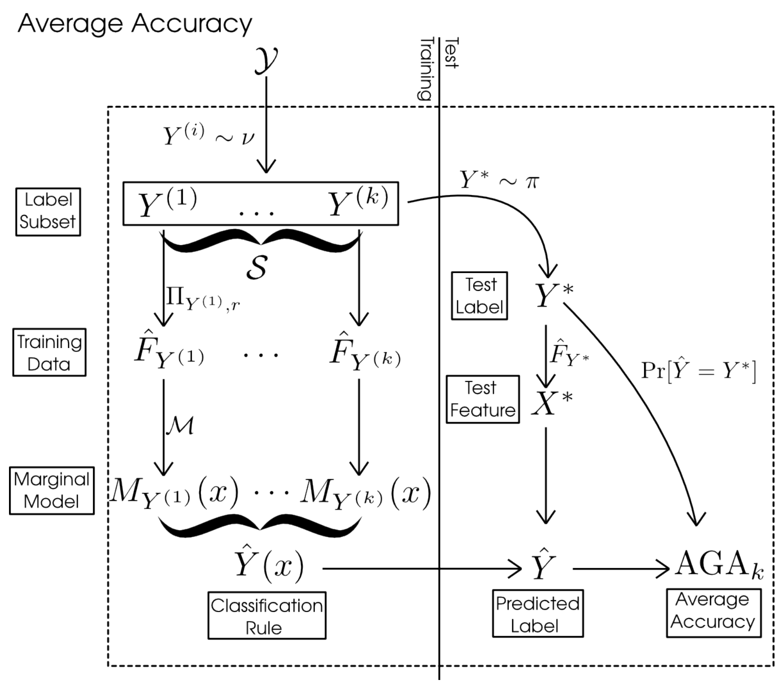


Figure 4: Average generalization accuracy

Having defined the average (generalization) accuracy for the randomized classification task, we begin to develop the theory of how to *estimate* the average accuracy in the next section.

# 3 Estimation of average accuracy

Suppose we have training and test data for a classification task $P_1$ with $k_1$ classes, $r_1$-repeat training data and $r_2$-repeat test data. That is, we have label set $\mathcal{S}_1 = \{y^{(i)}\}_{i=1}^{k_1}$, as well as training sample $\hat{F}_{y^{(i)}}$ and test sample $(x_1^{(i)}, \ldots, x_{r_2}^{(i)})$ for $i = 1, \ldots, k_1$. How can we estimate the $k, r$-average accuracy of a marginal classifier $\mathcal{M}$ for arbitrary $k$ and $r$?

Let us start with the case $k = k_1$ and $r = r_1$. Then the answer is simple: construct the classification rule $h$ using marginal model $\mathcal{M}$ from the training data. Then the test accuracy of $h$ is an unbiased estimator of $\mathrm{AGA}_{k,r}$.

This follows from definition. Observe that $\mathrm{AGA}_{k_1,r_1}$ is the expected prediction risk for the classification rule $h$ for a randomized classification problem $P$ with $k_1$ classes and $r_1$-repeat training data. Of course, the classification task $P_1$ that we have been given is a random draw from the desired distribution of random classification problems. Therefore, the prediction risk of $h$ constructed from $P_1$ is unbiased for $\mathrm{AGA}_{k_1,r_1}$, and since test accuracy is unbiased for generalization accuracy, it follows that the test accuracy of $h$ is an unbiased estimator of $\mathrm{AGA}_{k,r}$, as we claimed.

In following sections, we consider more complicated cases where $k_1 \neq k$. However, before proceeding, let us first review the procedure for computing the test accuracy.

For any given test observation $x_j^{(i)}$, we obtain the predicted label $\hat{y}_j^{(i)}$ by computing the margin for each class,

$$M_{i,j,\ell} = \mathcal{M}(\hat{F}_{y^{(\ell)}})(x_j^{(i)}) = m_{y^{(\ell)}}(x_i^{(j)}),$$

for $\ell = 1, \ldots, k_1$, and by finding the class with the highest margin $M_{i,j,\ell}$,

$$\hat{y}_j^{(i)} = y^{(\mathrm{argmax}_\ell M_{i,j,\ell})}.$$

The test accuracy is the fraction of correct classification over test observations,

$$\mathrm{TA} = \frac{1}{r_2 k_1} \sum_{i=1}^{k_1} \sum_{j=1}^{r_2} I(\hat{y}_j^{(i)} = y^{(i)}). \tag{1}$$

For each test observation, define the ranks of the margins by

$$R_{i,j,\ell} = \sum_{m \neq \ell} I\{M_{i,j,\ell} \geq M_{i,j,m}\}.$$

Therefore, $\hat{y}_j^{(i)}$ is equal to $y^{(i)}$ if and only if $R_{i,j,i} = k_1$. Thus, an equivalent expression for test accuracy is

$$\mathrm{TA} = \frac{1}{r_2 k_1} \sum_{i=1}^{k_1} \sum_{j=1}^{r_2} I\{R_{iji} = k_1\}. \tag{2}$$

### 3.1 Subsampling method

Next, let us consider the case where $k < k_1$ and $r = r_1$. Define a classification problem $P_2$ with label set $\mathcal{S}_2$ obtained by sampling $k$ labels uniformly without replacement from $\mathcal{S}_1$. Let the training and test data for $P_2$ be obtained by taking the training data and test data from $P_1$ belonging to labels in $\mathcal{S}_1$. It follows that $P_2$ is a randomized classification task with $k$ labels, $r_1$-repeat training data and $r_2$-repeat test data. Therefore, by the previous argument, the test accuracy for a classification rule $h$ constructed using the training data in $P_2$ provides an unbiased estimate of $\text{AGA}_{k,r_1}$.

However, we can get a much better unbiased estimate of $\text{AGA}_{k,r_1}$ by averaging over the randomization of $\mathcal{S}_2$. Naïvely, this requires us to train and evaluate $\binom{k_1}{k}$ classification rules. However, due to the special structure of marginal classifiers, we do the computation in the same order of computation as evaluating a single classification rule (assuming that the computational bottleneck is in training the classifier.)

This is because the rank $R_{iji}$ of the correct label, $i$, for the $x_j^{(i)}$ allows us to determine how many subsets $\mathcal{S}_2$ will result in a correct classification. For example $x_j^{(i)}$, there are $R_{iji} - 1$ labels with a lower margin than the correct label $i$. Therefore, as long as one of the classes in $\mathcal{S}_2$ is $i$, and the other $k-1$ labels are from the set of $R_{iji} - 1$ labels with lower margin than $i$, the classification of $x_j^{(i)}$ will be correct. This implies that there are $\binom{R_{iji}-1}{k-1}$ such subsets $\mathcal{S}_2$ where $x_j^{(i)}$ is classified correctly, and therefore

$$\text{AverageTA}_{k,r_1} = \frac{1}{\binom{k_1}{k}} \frac{1}{r_2 k} \sum_{i=1}^{k_1} \sum_{j=1}^{r_2} \binom{R_{iji} - 1}{k - 1}. \tag{3}$$

# 4 Extrapolation

In this chapter, we continue the discussion of Chapter 2, but focus specifically on the the question of how to estimate the $k$-class average accuracy, $\text{AGA}_{k,r}$, based on data from a problem $P_1$ with $k_1 < k$ classes, and $r = r_1$-repeat training data. This problem of *prediction extrapolation* is especially interesting for a number of applied problems.

- Example 1: A researcher develops a classifier for the purpose of labelling images in 10,000 classes. However, for a pilot study, her resources are sufficient to tag only a smaller subset of these classes, perhaps 100. Can she estimate how well the algorithm work on the full set of classes based on an initial "pilot" subsample of class labels?

- Example 2: A neuroscientist is interested in how well the brain activity in various regions of the brain can discriminate between different classes of stimuli. Kay et al. 2008 obtained fMRI brain scans which record how a single subject's visual cortex responds to natural images. They wanted to know how well the brain signals could discriminate between different images. For a set of 1750 photographs, they constructed a classifier which achieved over 0.75 accuracy of classification. Based on exponential extrapolation, they estimate that it would take on the order of $10^{9.5}$ classes before the accuracy of the model drops below 0.10! A theory of performance extrapolation could be useful for the purpose of making such extrapolations in a more principled way.

- The stories just described can be viewed as a metaphor for typical paradigm of machine learning research, where academic researchers, working under limited resources, develop novel algorithms and apply them to relatively small-scale datasets. Those same algorithms may then be adopted by companies and applied to much larger datasets with many more classes. In this scenario, it would be convenient if one could simply assume that performance on the smaller-scale classification problems was highly representative of performance on larger-scale problems.

Previous works have shown that generalizing from a small set of classes to a larger one is not straightforward. In a paper titled "What does classifying more than 10,000 Image Categories Tell Us," Deng and co-authors compared the performance of four different classifiers on three different scales: a small-scale (1,000-class) problem, medium-scale (7,404-class) problem, and large-scale (10,184-class) problem (all from ImageNet.) They found that while the nearest-neighbor classifier outperformed the support vector machine classifier (SVM) in the small and medium scale, the ranking switched in the large scale, where the SVM classifier outperformed nearest-neighbor. As they write in their conclusion, "we cannot always rely on experiments on small datasets to predict performance at large scale." Theory for performance extrapolation may therefore reveal models with bad scaling properties in the pilot stages of development.

However, in order to formally develop a method for extrapolating performance, it is necessary to specify the model for how the small-scale problem is related to the larger-scale problem. The framework of randomized classification introduced in Chapter 2 is one possible choice for such a model: the small-scale problem and large-scale problem are linked by having classes drawn from the same population.

The rest of the chapter is organized as follows. We begin by continuing to analyze the average accuracy $\text{AGA}_{k,r}$, which results in an explicit formula for the average accuracy. The formula reveals that all of the information needed to compute the average accuracy is contained in a one-dimensional function $\bar{D}(u)$, and therefore that estimation of the average accuracy can be accomplished via estimation of the unknown function $\bar{D}(u)$. This allows the development of a class of unbiased estimators of $\bar{D}(u)$, presented in section 4.3 given the assumption of a known parametric form for $\bar{D}(u)$. We analyze the performance of the estimator in both the well-specified and misspecified case. We demonstrate our method to a face-recognition example in section 5. Additionally, in Chapter 5 comparison of the estimator to an alternative, information-theory based estimator in simulated and real-data examples.

## 4.1 Toy example

Let us first illustrate using a toy example the computation of the average risk, and preview the theory for extrapolating the average risk.

Let $(Y, X)$ have a bivariate normal joint distribution,

$$(Y, X) \sim N\left(\begin{pmatrix}0\\0\end{pmatrix}, \begin{pmatrix}1 & \rho\\ \rho & 1\end{pmatrix}\right),$$

as illustrated in figure 5(a). Therefore, for a given randomly drawn label $Y$, the conditional distribution of $X$ for that label is univariate normal with mean $\rho Y$ and variance $1 - \rho^2$:

$$X|Y = y \sim N(\rho Y, 1 - \rho^2).$$

Supposing we draw $k = 3$ labels $y_1, y_2, y_3$, the classification problem will be to assign a test instance $X^*$ to the correct label. The test instance would be drawn from the three-class mixture,

$$X^* \sim \frac{1}{k}\sum_{i=1}^{k} p(x|y_i),$$

as illustrated in figure 5(b, top). In this toy example, we ignore the issue of training a classifier from sampled data, and instead assume that we have access to the *Bayes classification rule*, or optimal classification rule. The Bayes rule assigns $X^*$ to the class with the highest density $p(x|y_i)$, as illustrated by figure 5(b, bottom).

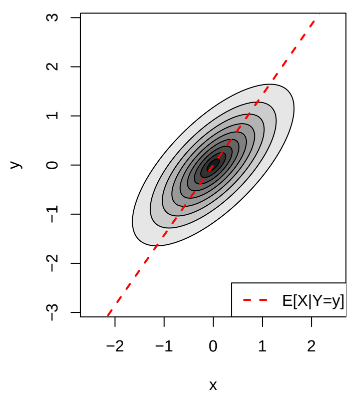


(a)

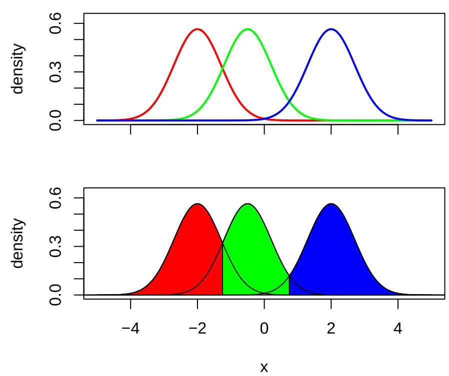


(b)

Figure 5: (a) The joint distribution of $(X, Y)$ is bivariate normal with correlation $\rho = 0.7$. (b) A typical classification problem instance from the bivariate normal model with $k = 3$ classes. Top: the conditional density of $X$ given label $Y$, for $Y = \{y_1, y_2, y_3\}$. Bottom: the Bayes classification regions for the three classes.

The risk of the Bayes rule for any label set $\{y_1, \ldots, y_k\}$ is given by

$$\text{Risk}(y_1, \ldots, y_k) = \frac{1}{k} \sum_{i=1}^{k} \Pr_{X \sim p(x|y_i)} [p(X|y_i) = \max_{j=1}^{k} p(X|y_j)].$$

We numerically computed $\text{Risk}(y_1, \ldots, y_k)$ for randomly drawn labels $Y_1, \ldots, Y_k \stackrel{iid}{\sim} N(0, 1)$; the distributions of $\text{Risk}(Y_1, \ldots, Y_k)$ for $k = 2, \ldots, 10$ are illustrated in figure 6. The $k$-class average risk, $\text{AvRisk}_k$, in this case, is given by

$$\text{AvRisk}_k = \mathbf{E}[\text{Risk}(Y_1, \ldots, Y_k)]$$

for $Y_1, \ldots, Y_k \stackrel{iid}{\sim} N(0, 1)$. The theory presented in the rest of the section deals with how to analyze the average risk $\text{AvRisk}_k$ as a function of $k$. We now proceed to preview some selected aspects of the theory for the toy example.

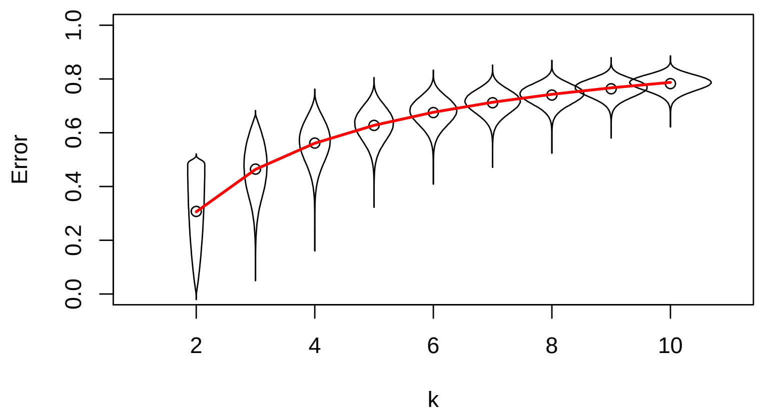


Figure 6: The distribution of the classification risk for $k = 2, 3, \ldots, 10$ for the bivariate normal model with $\rho = 0.7$. Circles indicate the average classificatin risk; the red curve is the theoretically computed average risk.

For a given test instance $X^*$ drawn from the label $Y^*$, the closer that $X^*$ is to the center of the correct class distribution, $\rho Y^*$, the more likely it is to be classified correctly. Based on this concept, we define the *conditional accuracy* function $U_x(y)$, which gives the conditional probability that a test instance $(Y_1, X_1)$ will be classified correctly in the two-class classification problem. One can therefore think of $U_x(y)$ as measuring the "strength" of the pair $(y, x)$, with stronger pairs being more likely to be classified correctly. Since in the two-class problem, there is one incorrect class label $Y_2$, the conditional accuracy in this case is simply the probability that $\rho Y_2$ is closer to $X_1$ than $\rho Y_1$. Therefore, in this toy example, we can give an explicit formula

$$\begin{aligned}
U_x(y) &= \Pr[p(x|y) < p(x|Y)] \\
&= \Pr[|\rho Y - x| < |\rho y - x|] \\
&= \Phi\left(\frac{x + |\rho y - x|}{\rho}\right) - \Phi\left(\frac{x - |\rho y - x|}{\rho}\right),
\end{aligned}$$

where $\Phi$ is the standard normal cumulative distribution function. Figure 7(a) illustrates the level sets of the function $U_x(y)$. The highest values of $U_x(y)$ are near the line $x = \rho y$ corresponding the to conditional mean of $X|Y$: as one moves farther from the line, $U_x(y)$ decays. Note however that large values of $(y, x)$ (with the same sign) result in larger values of $U_x(y)$

since it becomes unlikely for $Y_2 \sim N(0,1)$ to exceed $Y_1 = y$.

Now define the random variable $U = U_X(Y)$ for $(X, Y)$ drawn from the joint distribution. An important object in our theory is the cumulative distribution function [2] of $U$, written as

$$\bar{D}(u) = \Pr[U \leq u].$$

The function $\bar{D}$ is illustrated in figure 7(b) for the current example with $\rho = 0.7$. The red curve in figure 6 was computed using the formula

$$\text{AvRisk}_k = (k-1) \int \bar{D}(u) u^{k-2} du.$$

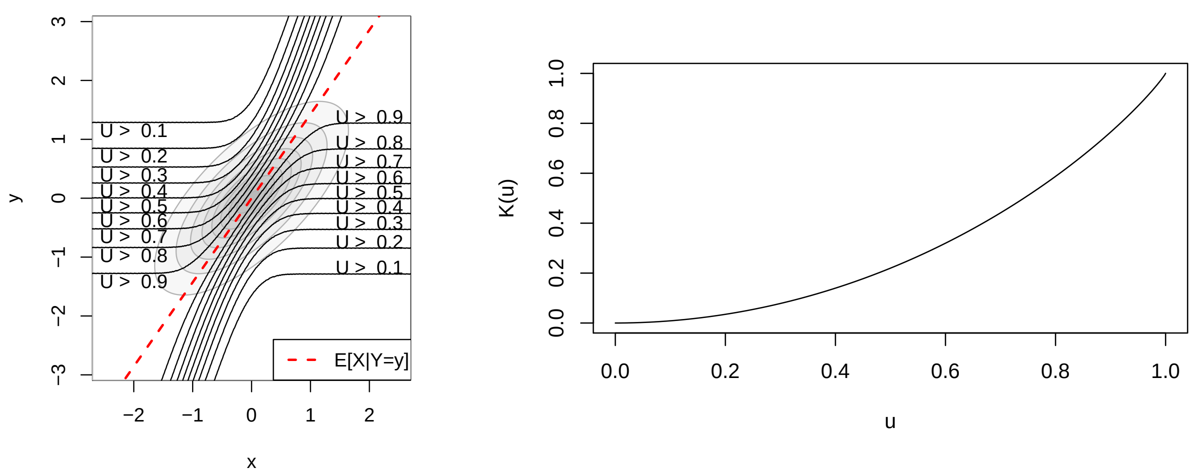


(a) (b)

Figure 7: (a) The level curves of the function $U_x(y)$ in the bivariate normal model with $\rho = 0.7$. (b) The function $\bar{D}(u)$, which gives the cumulative distribution function of the random variable $U_Y(X)$.

It is illuminating to consider how the average risk curves and the $\bar{D}(u)$ functions vary as we change the parameter $\rho$. Higher correlations $\rho$ lead to lower classification risk, as seen in figure 8(a), where the risk curves are

[2] Note however that $\bar{D}(u)$ is only defined as the cumulative distribution function of $U$ in the class of zero-one loss–the definition for general cost functions is somewhat more involved, as we will see.

shifted downward as $\rho$ increases from 0.3 to 0.9. The conditional accuracy $U_y(x)$ tends to be higher on average as well, which leads to lower values of the cumulative distribution function–as we see in figure 8(b), where the function $\bar{D}(u)$ becomes smaller as $\rho$ increases.

In section **??**, when we consider approximating $\bar{D}(u)$ by polynomials, or some other function basis, it becomes relevant to consider how well $\bar{D}(u)$ can be approximated by such bases in realistic problems. We see in figure 8(c) that, at least in this toy problem, $\bar{D}(u)$ is well-aproximated by low-order polynomials. However, the approximation becomes less adequate as $\rho$ increases. We can see visually why this is the case: as $\rho$ increases, the curvature of $\bar{D}(u)$ near $u = 1$ increases. Hence, higher-degree polynomials become needed to capture the behavior near $u = 1$. More generally, we observe that in cases where classes are relatively well-separated, it becomes necessary to use increasingly precise approximations in order to extrapolate the average risk.

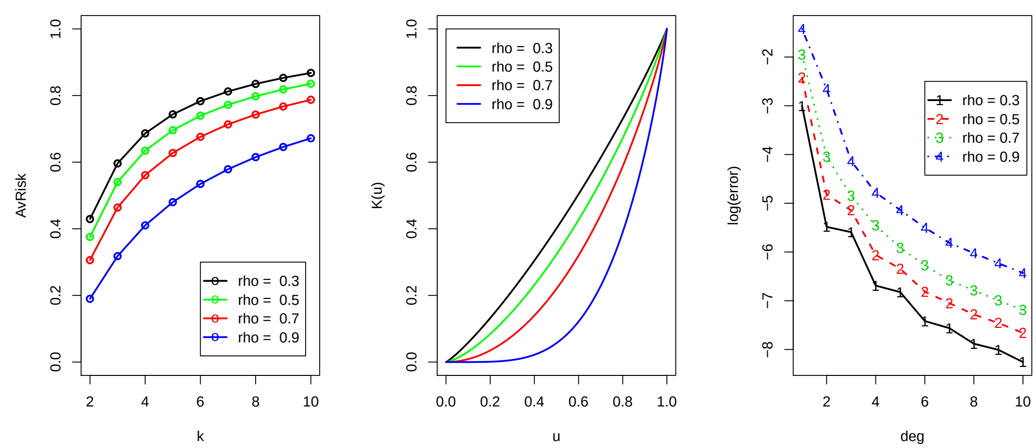


(a) (b) (c)

Figure 8: The (a) average risk, (b) $\bar{D}(u)$ function for $k = 2, \ldots, 7$ for the bivariate normal model with $\rho \in \{0.3, 0.5, 0.7, 0.9\}$. (c) The $d$-degree $\ell_\infty$ polynomial approximation error for $\bar{D}(u)$ for the bivariate normal model with $\rho \in \{0.3, 0.5, 0.7, 0.9\}$.

## 4.2 Analysis of average risk

The result of our analysis is to expose the average accuracy $\mathrm{AGA}_{k,r}$ as the weighted average of a function $\bar{D}(u)$, where $\bar{D}(u)$ is independent of $k$, and where $k$ only changes the weighting. The result is stated as follows.

**Theorem 4.1** *Suppose $\pi$, $\{F_y\}_{y\in\mathcal{Y}}$ and marginal classifier $\mathcal{F}$ satisfy the tie-breaking condition. Then, under the definitions* (5) *and* (8)*, we have*

$$AGA_{k,r} = 1 - (k-1)\int \bar{D}(u)u^{k-2}du. \tag{4}$$

The tie-breaking condition referred in the theorem is defined as follows.

- *Tie-breaking condition*: for all $x \in \mathcal{X}$, $\mathcal{M}(\hat{F}_Y)(x) = \mathcal{M}(\hat{F}_{Y'})(x)$ with zero probability for $Y, Y'$ independently drawn from $\pi$.

The tie-breaking condition is a technical assumption which allows us to neglect the specification of a tie-breaking rule in the case that margins are tied. In practice, one can simply break ties randomly, which is mathematically equivalent to adding a small amount of random noise $\epsilon$ to the function $\mathcal{M}$.

As we can see from Figure 4, the average accuracy is obtained by averaging over four randomizations:

A1. Drawing the label subset $\mathcal{S}$.

A2. Drawing the training dataset.

A3. Drawing $Y^*$ uniformly at random from $\mathcal{S}$.

A4. Drawing $X^*$ from $F_{X^*}$.

Our strategy is to analyze the average accuracy by means of *conditioning on* the true label and its training sample, $(y^*, \hat{F}_{y^*})$, and the test feature $x^*$ while *averaging* over all the other random variables. Define the *conditional accuracy* $\mathrm{CondAcc}_k((y^*, \hat{F}_{y^*}), x^*)$ as

$$\mathrm{CondAcc}_k((y^*, \hat{F}_{y^*}), x^*) = \Pr[\mathrm{argmax}_{y\in\mathcal{S}}\mathcal{M}(\{\hat{F}_y\})(X^*) = Y^*|Y^* = y^*, X^* = x^*, \hat{F}_{Y^*} = \hat{F}_{y^*}].$$

Figure 9 illustrates the variables which are fixed under conditioning and the variables which are randomized. Compare to figure 4.

Without loss of generality, we can write the label subset $\mathcal{S} = \{Y^*, Y^{(1)}, \ldots, Y^{(k-1)}\}$. Note that due to independence, $Y^{(1)}, \ldots, Y^{(k-1)}$ are still i.i.d. from $\pi$ even conditioning on $Y^* = y^*$. Therefore, the conditional risk can be obtained via the following alternative order of randomizations:

C0. Fix $y^*, \hat{F}_y^*$, and $x^*$. Note that $M_{y^*}(x^*) = \mathcal{M}(\hat{F}_{y^*})(x^*)$ is also fixed.

C1. Draw the *incorrect labels* $Y^{(1)}, \ldots, Y^{(k)}$ i.i.d. from $\pi$. (Note that $Y^{(i)} \neq y^*$ with probability 1 due to the continuity assumptions on $\mathcal{Y}$ and $\pi$.)

C2. Draw the training samples for the incorrect labels $\hat{F}_{Y^{(1)}}, \ldots, \hat{F}_{Y^{(k-1)}}$. This determines

$$\hat{Y} = \text{argmax}_{y \in \mathcal{S}} M_y(x^*)$$

and hence, whether or not the classification is correct for $(x^*, y^*)$

Compared to four randomization steps for the average risk, we have essentially conditioned on steps A3 and A4 and randomized over steps A1 and A2.

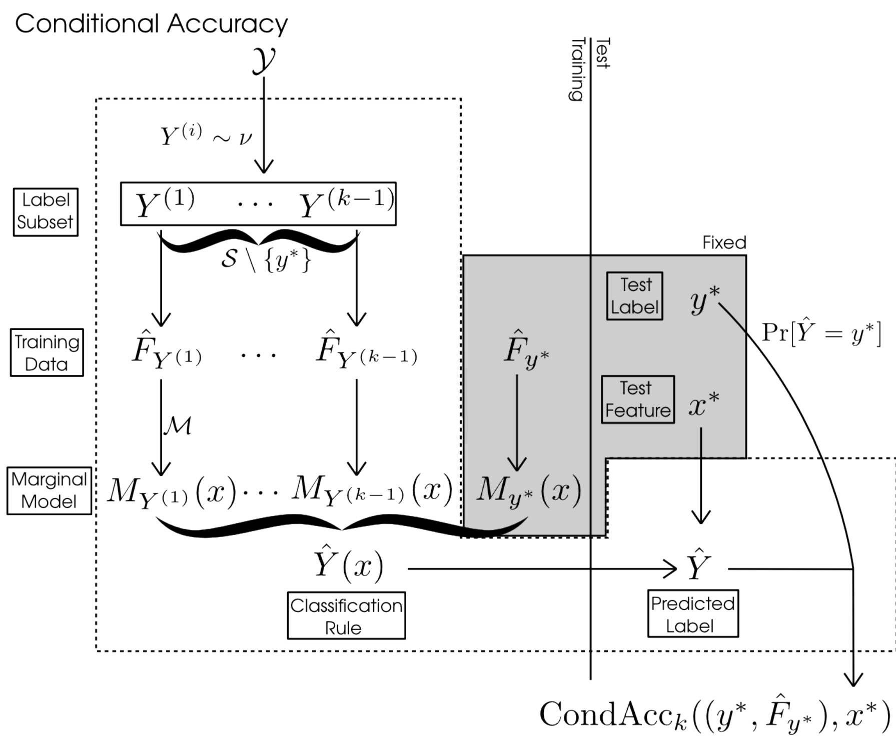


Figure 9: Conditional accuracy

Now, in order to analyze the $k$-class behavior of the conditional accuracy, we begin by considering the *two-class* situation.

In the two-class situation, we have a true label $y^*$, a training sample $\hat{F}_{y^*}$, and one incorrect label, $Y$. Define the *U-function* $U_{x^*}(y^*, \hat{F}_{y^*})$ as the conditional accuracy (the probability of correct classification) in the two-class case. The classification is correct if the margin $M_{y^*}(x^*)$ is greater than the margin $M_Y(x^*)$, and incorrect otherwise. Since we are fixing $x^*$ and $(y^*, \hat{F}_{y^*})$, the probability of correct classification is obtained by taking an expectation:

$$U_{x^*}(y^*, \hat{F}_{y^*}) = \Pr[M_{y^*}(x^*) > \mathcal{M}(\hat{F}_Y)(x^*)] \tag{5}$$

$$= \int_{\mathcal{Y}} I\{M_{y^*}(x^*) > \mathcal{M}(\hat{F}_y)(x)\} d\Pi_{y,r}(\hat{F}_y) d\pi(y). \tag{6}$$

See also figure 10 for an graphical illustration of the definition.

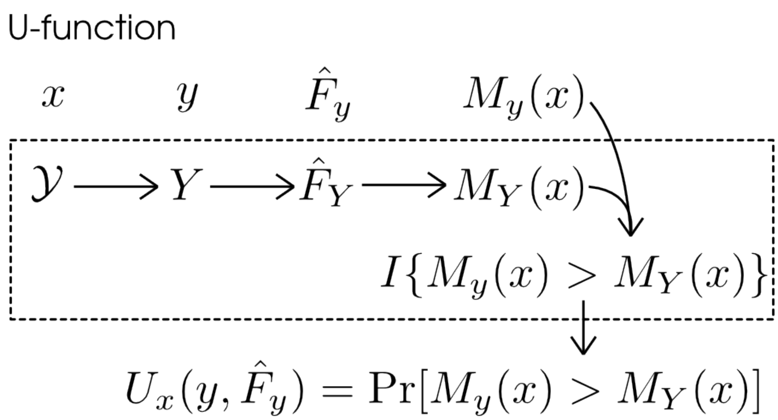


Figure 10: U-functions

An important property of the U-function, and the basis for its name, is that the random variable $U_x(Y, \hat{F}_Y)$ for $Y \sim \pi$ and $\hat{F}_Y \sim \Pi_{Y,r}$ is uniformly distributed for all $x \in \mathcal{X}$. This is proved in Lemma **??** in Appendix C.

Now, we will see how the U-function allows us to understand the $k$-class case. Suppose we have true label $y^*$ and incorrect labels $Y^{(1)}, \ldots, Y^{(k-1)}$. Note that the U-function $U_{x^*}(y, \hat{F}_y)$ is monotonic in $M_y(x^*)$. Therefore,

$$\hat{Y} = \text{argmax}_{y \in \mathcal{S}} M_y(x^*) = \text{argmax}_{y \in \mathcal{S}} U_{x^*}(y, \hat{F}_y).$$

Therefore, we have a correct classification if and only if the U-function value for the correct label is greater than the maximum U-function values for the incorrect labels:

$$\Pr[\hat{Y} = y^*] = \Pr[U_{x^*}(y^*, \hat{F}_{y^*}) > \max_{i=1}^{k-1} U_{x^*}(Y^{(i)}, \hat{F}_{Y^{(i)}})] = \Pr[u^* > U_{max}].$$

where $u^* = U_{x^*}(y^*, \hat{F}_{y^*})$ and $U_{max,k-1} = \max_{i=1}^{k-1} U_{x^*}(Y^{(i)}, \hat{F}_{Y^{(i)}})$. But now, observe that we know the distribution of $U_{max,k-1}$! Since $U_{x^*}(Y^{(i)}, \hat{F}_{Y^{(i)}})$ are i.i.d. uniform, we know that

$$U_{max,k-1} \sim \text{Beta}(k-1, 1). \tag{7}$$

Therefore, in the general case, the conditional accuracy is

$$\text{CondAcc}_k((y^*, \hat{F}_{y^*}), x^*) = \Pr[U_{max} > u^*] = 1 - \int_{u^*}^1 (k-1)u^{k-2}du.$$

Now the average accuracy can be obtained by integrating over the distribution of $U^* = U_{x^*}(y^*, \hat{F}_{y^*})$, which we state in the following proof of theorem 4.1.

**Proof of Theorem 4.1**. We have

$$\begin{aligned}\text{AGA}_{k,r} &= \mathbf{E}[1 - \int_{U^*}^1 (k-1)u^{k-2}du] \\ &= 1 - \mathbf{E}[\int_0^1 I\{u \geq U^*\}(k-1)u^{k-2}du] \\ &= (k-1)\int_0^1 \Pr[U^* \leq u]u^{k-2}du.\end{aligned}$$

Or equivalently,

$$\text{AGA}_{k,r}((y^*, \hat{F}_{y^*}), x^*) = 1 - (k-1)\int \bar{D}(u)u^{k-2}du.$$

where $\bar{D}(u)$ denotes the cumulative distribution function of $U^*$ on $[0, 1]$:

$$\bar{D}(u) = \Pr[U_{x^*}(y^*, \hat{F}_{y^*}) \leq u]. \tag{8}$$

We have expressed the average risk expressed as a weighted integral of a certain function $\bar{D}(u)$ defined on $u \in [0, 1]$. We have clearly isolated the part of the average risk which is independent of $k$–the univariate function $\bar{D}(u)$, and the part which is dependent on $k$–which is the density of $U_{max}$.

In section 4.3, we will develop estimators of $\bar{D}(u)$ in order to estimate the $k$-class average risk.

Having this theoretical result allows us to understand how the expected $k$-class risk scales with $k$ in problems where all the relevant densities are known. However, applying this result in practice to estimate Average Risk$_k$ requires some means of estimating the unknown function $\bar{D}$–which we discuss in the following.

## 4.3 Estimation

Now we address the problem of estimating $\text{AGA}_{k_2,r_1}$ from data. As we have seen from Theorem 4.1, the $k$-class average accuracy of a marginal classifier $\mathcal{M}$ is a functional of a object called $\bar{D}(u)$, which depends marginal model $\mathcal{M}$ of the classifier, the joint distribution of labels $Y$ and features $X$ when $Y$ is drawn from the sampling density $\nu$.

Therefore, the strategy we take is to attempt to estimate $\bar{D}$ for then given classification model, and then plug in our estimate of $\bar{D}$ into the integral (4) to obtain an estimate of $\text{AGA}_{k_2,r_{train}}$.

Having decided to estimate $\bar{D}$, there is then the question of what kind of model we should assume for $\bar{D}$. In this work, we assume that some parametric model[3] is available for $\bar{D}$.

Let us assume the linear model

$$\bar{D}(u) = \sum_{\ell=1}^{m} \beta_\ell h_\ell(u), \tag{9}$$

where $h_\ell(u)$ are known basis functions, and $\beta$ are the model parameters to be estimated. We can obtain *unbiased* estimation of $\text{AGA}_{k_2,r_{train}}$ via the unbiased estimates of $k$-class average risk obtained from (3).

If we plug in the assumed linear model (9) into the identity (4), then we get

$$\begin{aligned}
1 - \text{AGA}_{k,r_{train}} &= 1 - (k-1) \int \bar{D}(u) u^{k-2} du && (10)\\
&= 1 - (k-1) \int_0^1 \sum_{\ell=1}^{m} \beta_\ell h_\ell(u) u^{k-2} du && (11)\\
&= 1 - \sum_{\ell=1}^{m} \beta_\ell H_{\ell,k} && (12)
\end{aligned}$$

where

$$H_{\ell,k} = (k-1) \int_0^1 h_\ell(u) u^{k-2} du. \tag{13}$$

The constants $H_{\ell,k}$ are moments of the basis function $h_\ell$: hence we call this method the *moment method.* Note that $H_{\ell,k}$ can be precomputed numerically for any $k \geq 2$.

[3]While a nonparametric approach may be more ideal, we leave this to future work.

Now, since the test accuracies $\mathrm{TA}_k$ are unbiased estimates of $\mathrm{AGA}_{k,r_{train}}$, this implies that the regression estimate

$$\hat{\beta} = \mathrm{argmin}_\beta \sum_{k=2}^{k_1} w_k \left( (1 - \mathrm{TA}_k) - \sum_{\ell=1}^{m} \beta_\ell H_{\ell,k} \right)^2$$

is unbiased for $\beta$, under any choice of positive weights $w_k$. The estimate of $\mathrm{AGA}_{k_2,r_1}$ is similarly obtained from (12), via

$$\widehat{\mathrm{AGA}_{k_2,r_1}} = 1 - \sum_{\ell=1}^{m} \hat{\beta}_\ell H_{\ell,k_2}. \tag{14}$$

# 5 Examples

## 5.1 Facial recognition example

From the "Labeled Faces in the Wild" dataset (Huang et al. 2007), we selected 1672 individuals with at least 2 face photos. We form a dataset consisting of photo-label pairs $(\vec{z}_j^{(i)}, y^{(i)})$ for $i = 1, \ldots, 1672$ and $j = 1, 2$ by randomly selecting 2 face photos for each of the 1672 individuals.

We implement a face recognition system based on one nearest-neighbor and OpenFace (Amos, Ludwiczuk, and Satyanarayanan 2016) for feature extraction. For each photo $\vec{z}$, a 128-dimensional feature vector $\vec{x}$ is obtained as follows.

1. The computer vision library DLLib is used to detect landmarks in $\vec{z}$, and to apply a nonlinear transformation to align $\vec{z}$ to a template.

2. The aligned photograph is downsampled to a $96 \times 96$ input, which is fed into a pre-trained deep convolutional neural network to obtain the 128-dimensional feature vector $\vec{x}$.

Therefore, we obtain feature-label pairs $(\vec{z}_j^{(i)}, y^{(i)})$ for $i = 1, \ldots, 1672$ and $j = 1, 2$.

The recognition system then works as follows. Suppose we want to perform facial recognition on a subset of the individuals, $I \subset \{1, \ldots, 1672\}$. Then, for all $i \in I$, we load one feature vector-label pair, into the system,

$(\vec{x}_1^{(i)}, y^{(i)})$. In order to identify a new photo $\vec{z}^*$, we obtain the feature vector $\vec{x}^*$, and guess the label $\hat{y}$ based on example with the minimal distance to $\vec{x}^*$,

$$\hat{y} = y^{(i^*)}$$

where

$$i^* = \text{argmin}_I d(\vec{x}, \vec{x}_1^{(i)}).$$

The test accuracy is assessed on the unused repeat for all individuals in $I$. Note that the assumptions of our estimation method are met in this example because one-nearest neighbor is a marginal classifier. One can define the margin functions as

$$(\mathcal{M}(\vec{x}))(\vec{x}^*) = -||\vec{x} - \vec{x}^*||^2.$$

However, $k$-nearest neighbor for $k > 1$ is not marginal.

While we can apply our extrapolation method to estimate the average accuracy for any number of faces $k$, it will not be possible to validate our estimates if we use the full dataset. Therefore, we take the average accuracies computed using the subsampling method (3) on the full dataset as a *ground truth* to compare to the average accuracy estimated from a *subsampled* dataset. Therefore, we simulate the problem of performance extrapolation from a database of $K$ faces by subsampling a dataset of size $K$ from the LFW dataset.

To do the performance extrapolation, we use a linear spline basis,

$$h_\ell(u) = \left[u - \frac{\ell - 1}{m}\right]_+$$

for $\ell = 1, \ldots, m$. Here we take $m = 10000$. We model the function $\bar{D}(u)$ as a non-negative linear combination of basis functions,

$$\bar{D}(u) = \sum_{\ell=1}^{m} \beta_\ell h_\ell(u),$$

with $\beta_\ell \geq 0$. The resulting estimated generalization accuracies, computed using (4), are plotted in Figure (11) (b). As we already mentioned, to assess the quality of the estimated average accuracy, we compare them to the 'ground truth' accuracy curve obtained by using all 1672 examples to compute the the average test risk.

To get an idea of the accuracy and variance of the accuracy curve estimates for varying sample sizes $K$, we repeat this procedure multiple times for $K \in \{100, 200, 400, 800\}$. The results, again compared to the ground truth computed from the full data set, are illustrated in figure 12.

a b

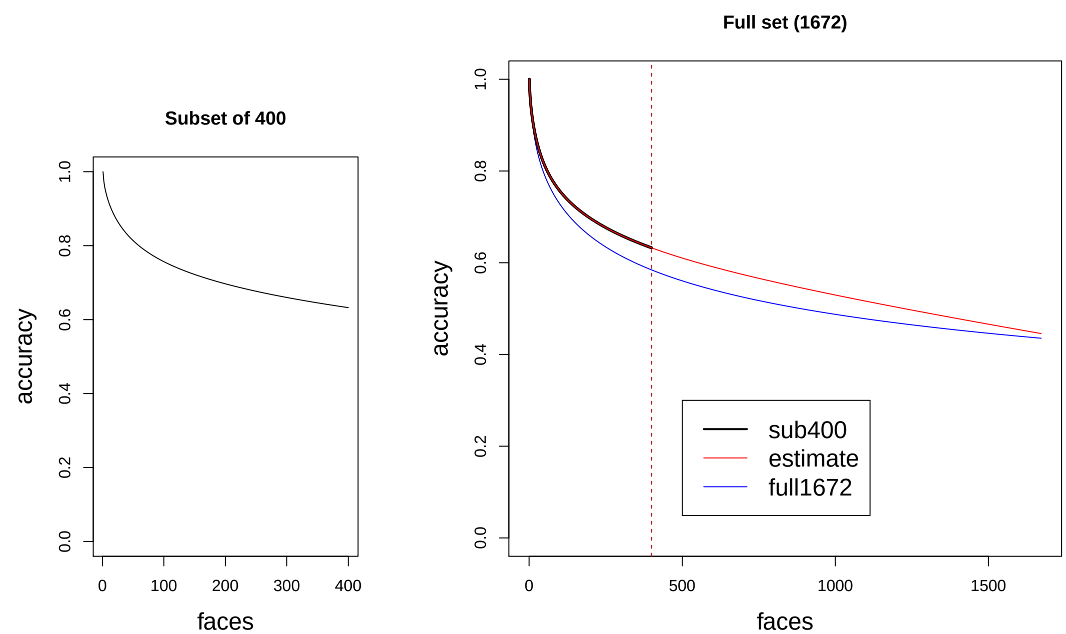


Figure 11: (a) The estimated average accuracy for $k = 2, \ldots, 400$ given a dataset of 400 faces subsampled from Labeled Faces in the Wild. (b) Estimated average accuracy for $k > 400$ on the same dataset, compared to the ground truth (average $k$-class test accuracy using all 1672 classes).

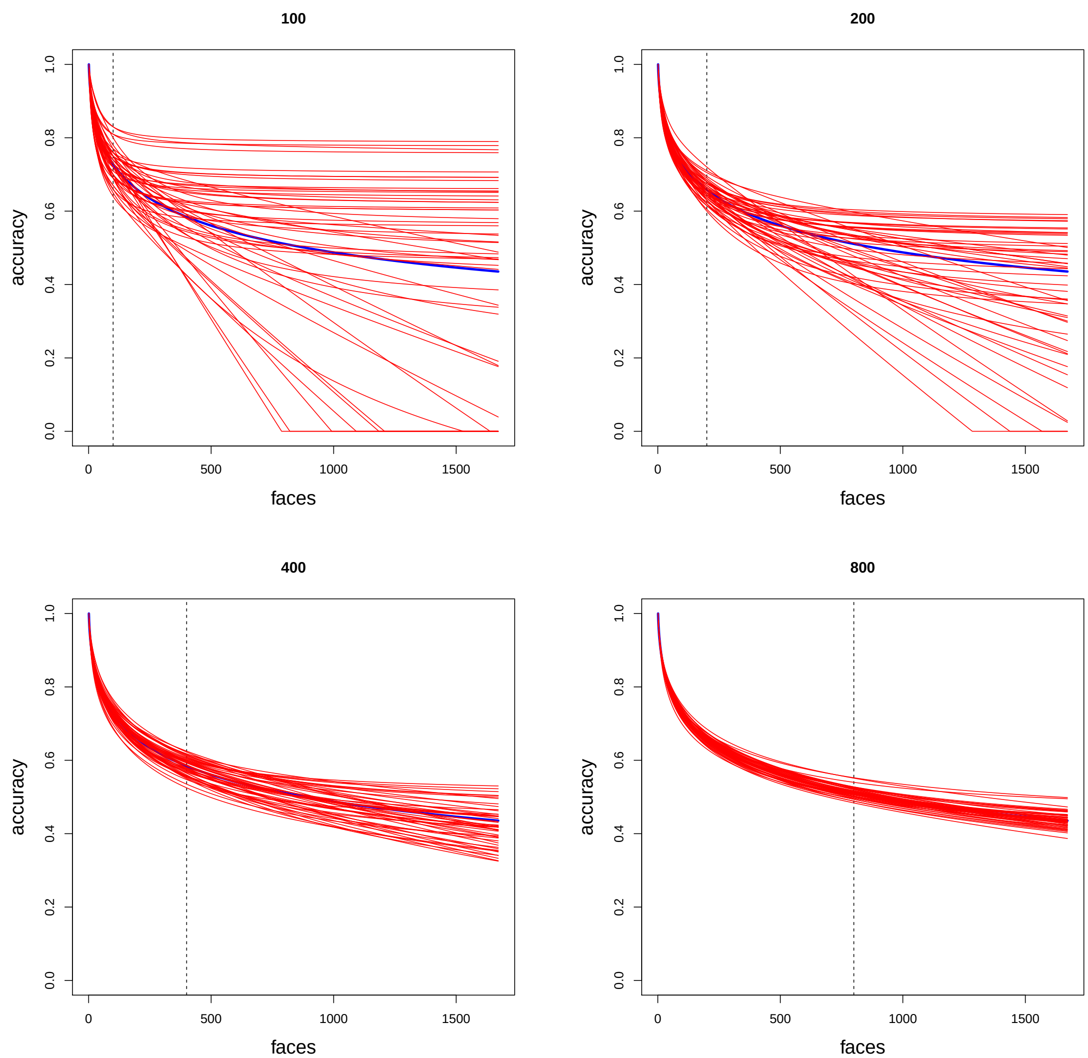


Figure 12: Estimated average accuracy using subsampled datasets of size $k$, compared to the ground truth (average $k$-class test accuracy using all 1672 classes).

| Classifier | Test 1-acc$^{(100)}$ | Test 1-acc$^{(400)}$ | 1-$\hat{AGA}_{400}$ |
|---|---|---|---|
| Naive Bayes | 0.217 | 0.399 | 0.501 |
| Logistic | 0.151 | 0.289 | 0.341 |
| SVM | 0.242 | 0.455 | 0.491 |
| $\epsilon$-NN | 0.209 | 0.409 | 0.621 |
| Deep neural net | 0.001 | 0.014 | 0.031 |

Table 1: Performance extrapolation: predicting the accuracy on 400 classes using data from 20 classes on a Telugu character dataset. $\epsilon = 0.002$ for $\epsilon$-nearest neighbors.

## 5.2 Telugu OCR example

While the previous example was a perfect fit to the assumptions of the framework, we also want to see how well the method works when some of the assumptions may be violated. Towards this end we apply performance extrapolation in an optical character recognition example (Achanta and Hastie 2015) for predicting the accuracy on 400 classes of Telugu characters from a subsample of size $K = 20$. We consider the use of five different classifiers: Naive Bayes, logistic regression, SVM, $\epsilon$-nearest neighbors[4], and a deep convolutional neural network[5]. Of the five classifiers, only Naive Bayes satisfies the marginal classifier assumption. Again, we compare the result of our model to the ground truth obtained by using the full dataset.

The results are displayed in Table 1. To our surprise, the worst absolute difference between ground truth and estimated average accuracy was in the case of Naive bayes ($|\delta| = 0.257$) which satisfies the marginal property. All other classifiers had absolute errors less than 0.2. It is also interesting to note that, even though Naive Bayes and $\epsilon$-nearest neighbors have the same test accuracy on the subset, that the predicted accuracy on 400 differs greatly between then (0.858 vs 0.400). Furthermore, the difference is in the right direction: Naive Bayes is predicted to work better on 400 classes than $\epsilon$-nearest neighbors, which appears to be the case based on the 400-class test accuracy.

While further work is still needed to better understand the performance of the proposed performance extrapolation method, both for marginal classifiers (which satisfy the theoretical assumptions) and non-marginal classifiers

[4] $k$-nearest neighbors with $k = \epsilon n$ for fixed $\epsilon > 0$

[5] The network architecture is as follows: `48x48-4C3-MP2-6C3-8C3-MP2-32C3-50C3-MP2-200C3-SM`.

(which do not), the results obtained in these two examples are encouraging in that sense that useful predictions were obtained both for marginal and non-marginal classifiers.

# References


Achanta, Rakesh and Trevor Hastie (2015). “Telugu OCR Framework using Deep Learning”. In: *arXiv preprint arXiv:1509.05962*.

Amos, Brandon, Bartosz Ludwiczuk, and Mahadev Satyanarayanan (2016). *OpenFace: A general-purpose face recognition library with mobile applications*. Tech. rep. CMU-CS-16-118, CMU School of Computer Science.

Huang, Gary B. et al. (2007). *Labeled Faces in the Wild: A Database for Studying Face Recognition in Unconstrained Environments*. Tech. rep. 07-49. University of Massachusetts, Amherst.

Kay, Kendrick N et al. (2008). “Identifying natural images from human brain activity.” In: *Nature* 452.March, pp. 352–355. ISSN: 0028-0836. DOI: `10.1038/nature06713`.

LeCun, Yann, Yoshua Bengio, and Geoffrey Hinton (2015). “Deep learning”. In: *Nature* 521.7553, pp. 436–444.